Complex Langevin equations and lattice gauge theory

Jon Flower, Steve W. Otto, and Sean Callahan
California Institute of Technology, Pasadena, California 91125
(Received 28 February 1986)

We consider the use of complex stochastic equations in the evaluation of ensemble averages. For a certain class of functions, it is shown how to relate averages over real parameters to those over complex degrees of freedom. We apply these techniques to the Abelian lattice gauge theory and discuss its extension to the non-Abelian case.

I. INTRODUCTION

A major problem in lattice gauge theories is the large size of the statistical errors in numerical Monte Carlo simulations. A new generation of supercomputers will certainly be of benefit in this regard, but the measurement of some quantities, such as exponentially small correlation functions, will remain frustrated if the usual "brute force" algorithms are applied. This paper discusses an alternative Monte Carlo technique which is potentially very powerful. It also applies not only to the correlation functions to be discussed here but also to other aspects of lattice gauge theory, e.g, dynamical fermions.

Specific examples of the problems to be addressed can be found in measurements of the properties of the heavy-quark–antiquark system with gauge group SU(3). Calculations of the static potential exist which have very small statistical errors.[1] However, attempts to measure the spin dependency of this potential,[2] and also the chromoelectric and magnetic flux densities[3] have suffered due to the noisiness of the observed signals when the $q\bar{q}$ pair are separated by more than a few lattice spacings.

A fundamental reason for this is that the procedures used can only generate configurations weighted by the vacuum action $F_{\mu\nu}F^{\mu\nu}$. Observables are then calculated as the correlation of some test plaquettes and a large current loop supposedly generated by the heavy quarks. This procedure is weak in the sense that one relies on the vacuum field configurations to spontaneously generate fields which have significant overlap with both our test probe and the $q\bar{q}$ current loop. Since this is not necessarily a high-probability occurrence large statistical errors may result.

A better procedure would be to somehow build the effect of the current loop into the action used to generate the fields. Then all the configurations would exhibit the properties of the $q\bar{q}$ system and the measured signals would be much stronger.

The difficulty with this prescription is that the quantity corresponding to the current loop is not positive definite, and so the usual, probabalistic algorithms such as the heat bath and Metropolis methods are not appropriate. In this paper, however, we discuss the application of the Langevin algorithm which still has formal solutions even for complex actions.[4–6]

The structure of the rest of this paper is as follows. In Sec. II the Langevin technique is introduced and it is shown how for a certain class of correlations, including most of those encountered in lattice gauge theories, the complex extension of the system is to be understood. In Sec. III we discuss the application of this algorithm to the Abelian U(1) theories in two and three dimensions and the numerical difficulties encountered. In Sec. IV the applicability of this technique to non-Abelian systems is discussed.

II. COMPLEX STOCHASTIC EQUATIONS

Consider first the case of a real action $S(x)$. We wish to calculate expectations in a probability distribution, $P(x)=e^{-S(x)}$, defined by

$$\langle f(x)\rangle = \frac{\int dx\, f(x)P(x)}{\int dx\, P(x)} \ . \tag{2.1}$$

The Langevin approach to this problem is to construct the associated stochastic differential equation (SDE) to the probability distribution $P(x)$:

$$d_S x = \frac{1}{P(x)}\frac{dP(x)}{dx}dt + \sqrt{2}\, dw(t) \ , \tag{2.2}$$

where $dw(t)$ is a normalized Brownian motion. To solve this equation one introduces a fictitious time t and discretizes to some order in δt. In this paper we use the first-order form

$$x(t+\delta t)-x(t)=\left[\frac{1}{P(x(t))}\frac{dP(x(t))}{dx}\right]\delta t+\sqrt{2\delta t}\,\eta \ , \tag{2.3}$$

where η is a Gaussian random number of mean zero and unit variance. This particular discretization corresponds to the Itô form of the SDE while (2.2) is in Stratonovitch form. The connection between these two is achieved by the Zakai-Wong correction (e.g., Ref. 7). For the type of systems to be considered here, however, in which the Brownian motion in (2.2) is multiplied by a constant, the two forms are identical and so for the rest of this paper we shall not distinguish between them.

Equation (2.2) describes the evolution of paths $x(t)$ whose probability density, $p(x(t),t)$ satisfies a Fokker-Planck equation in terms of the action $S(x)$:

$$\frac{\partial p(x,t)}{\partial t}=\frac{\partial}{\partial x}\left[\frac{\partial S}{\partial x}p\right]+\frac{\partial^2 p}{\partial x^2}\ . \tag{2.4}$$

Solutions to this equation are of the form

$$P(x,t)=\sum_{n=1} p_n(x,t)e^{-\lambda_n t}+e^{-S(x)} \tag{2.5}$$

and it can be shown (e.g., Ref. 8) that the eigenvalues satisfy the condition $\lambda_n>0$ for all $n\geq 1$. Thus all solutions $q(x,t)$ of (2.4) satisfy

$$\lim_{t\to\infty} q(x,t)=P(x)=e^{-S(x)}\ . \tag{2.6}$$

The ergodicity property then allows us to calculate ensemble averages such as (2.1) by

$$\langle f(x)\rangle=\lim_{T\to\infty}\frac{1}{T}\int_0^T dt\, f(x(t,x_0))\ , \tag{2.7}$$

where $x(t,x_0)$ is the solution of (2.2) at time t given an initial value x_0 at $t=0$.

The possibility to be considered is the case where $S(x)$ is a complex-valued function of x. If (2.2) holds then it shows that the variable x must itself become complex. In this case, however, it is unclear exactly what expression corresponds to (2.1). In Appendix A we show that for a certain class of functions, namely those which are entire and periodic in the sense that

$$f(z+2\pi)=f(z),\quad z=x+iy\ , \tag{2.8}$$

then the expression (2.1) becomes simply

$$\langle f\rangle=\frac{\int_{\mathbb{C}} dz\, f(z)P(z)}{\int_{\mathbb{C}} dz\, P(z)}\ , \tag{2.9}$$

where $P(z)$ and $f(z)$ are the analytic continuations of $P(x)$ and $f(x)$ and the range of integration is extended to the whole complex plane.

In this case we are entitled to replace (2.2) and (2.4) by their analytic continuations. The question of convergence, answered in the real case by (2.5), is rather more difficult, however, since the eigenvalues λ_n are no longer strictly positive. In the case where the imaginary part of $S(x)$ is small it can be shown that the eigenvalues λ_n all have real parts greater than zero which is enough to guarantee convergence,[9] but a more general theorem is unavailable.

III. ABELIAN LATTICE GAUGE THEORY

As an aid to understanding these techniques we begin with U(1) lattice gauge theory. This is a nontrivial theory but has the advantage of greater computational simplicity than the non-Abelian theories and also the existence of certain analytic results for comparison purposes. The particular correlation function to be measured is that between a large current loop W and a single orientable test plaquette P. In this study we confine attention to plaquettes lying in the plane of the loop W. This corresponds to measuring the squared energy density in the electric field parallel to the axis joining the charges. (See Fig. 1.)
The relevant path integral is

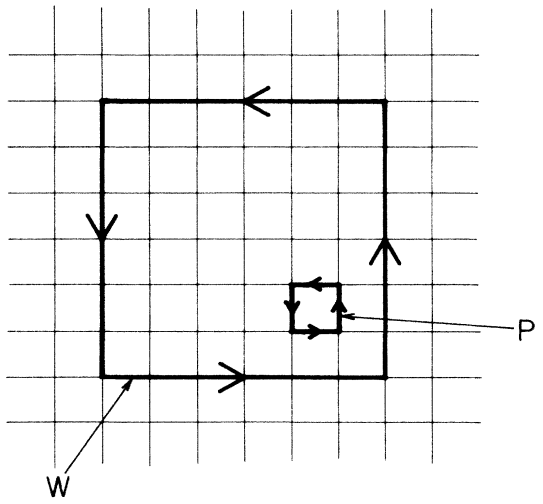

FIG. 1. The relative positioning of the Wilson loop W and plaquette P used to measure the squared energy density in the electric field.

$$\langle C_{WP}\rangle=\frac{\int[d\theta]e^{i\theta_l\delta_{l\in P}}e^{i\theta_m\delta_{m\in W}}e^{S}}{\int[d\theta]e^{i\theta_m\delta_{m\in W}}e^{S}}\ , \tag{3.1}$$

where $\delta_{m\in W}$ and $\delta_{l\in P}$ are used to pick out the links occurring in the loop W and plaquette P, respectively. The action S is the conventional Wilson action

$$S=\beta\sum_{\text{plaquettes},n}\cos\theta_{\mu\nu}(n) \tag{3.2}$$

and $\theta_{\mu\nu}$ is the path-ordered plaquette angle

$$\theta_{\mu\nu}=\theta_\mu(n)+\theta_\nu(n+\hat{\mu})-\theta_\mu(n+\hat{\nu})-\theta_\nu(n)\ . \tag{3.3}$$

As explained in the Introduction, we wish to include the effects of the current loop W in the action used to update the fields. Thus for the update of a particular link variable θ_m we must simulate the complex distribution

$$P(\theta_m)d\theta_m=\exp\left[\beta\sum_{j=1}^{2(d-1)}\cos(\theta_m+E_j)+i\delta_{m\in W}\theta_m\right]d\theta_m \tag{3.4}$$

(in d dimensions) where E_j is the jth "environment" associated with link m.

This leads to the SDE

$$d\theta_m=\left[\begin{array}{c}\displaystyle\sum_{j-1}^{2(d-1)}\cos(\theta_m+E_j)\\ -\beta\dfrac{}{\displaystyle\sum_{j=1}^{2(d-1)}\sin(\theta_m+E_j)}+i\delta_{m\in W}\end{array}\right]dt+\sqrt{2}\,dw(t)\ . \tag{3.5}$$

As has been observed previously[10] there are numerical problems with this sort of equation. In particular the trigonometric functions grow exponentially as distance from the real axis increases causing numerical overflows. Previous authors[4,11] have just truncated paths which wan-

dered too far from the real axis but this approach is unsuitable in lattice gauge calculations where considerable computation is required to generate lattice configurations—discarding an entire system when the imaginary part of one of the links becomes too large would be unworkable.

Consider, however, a generalized SDE

$$dx = B(x)dt + D(x)dw(t) \tag{3.6}$$

with the first-order discretization

$$x(t+\delta t) = x(t) + B(x)\delta t + D(x)\sqrt{2\delta t}\,\eta\ . \tag{3.7}$$

The criterion for accurate numerical simulation of this equation is that the time step δt must be chosen to satisfy

$$|D(x)| \gg |B(x)|(\delta t)^{1/2}\ . \tag{3.8}$$

In our numerical simulations, therefore, the time step is dynamically chosen to satisfy this constraint. Paths still exist which travel far into the complex plane since the system is ergodic, but they are now evolved in a controlled manner and remain within a bounded area rather than heading off to infinity.

The dynamical time-stepping algorithm is as follows. Say, for example, that we wish to evolve the system from Langevin time T to $T+\delta T$. Denote by $T_i \in [T, T+\delta T]$ the Langevin time to which link i has evolved. Then a lattice update is a series of sweeps through all the sites updating by δt_i chosen according to

$$\delta t_i = \min(T+\delta T - T_i, t_\Delta)\ , \tag{3.9}$$

where t_Δ is defined by (Δ is some predefined value, let us say 0.01)

$$(t_\Delta)^2 = \frac{|D(x(t))|^2}{|B(x(t))|^2}\Delta^2\ . \tag{3.10}$$

This constrains the individual links to evolve according to the constraint (3.8). This procedure is repeated until all sites have been evolved to $T+\delta T$.

This raises an interesting issue for the execution of this algorithm on parallel computers. A concurrent implementation could have load-balancing difficulties since some of the links require more updating "hits" than others. Our experience, however, shows that the areas where this is the case are few in number and small in size. Thus the extra calculation required is small by comparison with the total amount of work on any update. It is also possible, by suitable choice of the input parameters δT and Δ, to make small the number of extra "hits" required.

The results of simulations in two dimensions are shown in Figs. 2 and 3. They represent the correlations of a plaquette with a 5×5 Wilson loop. The theory is analytically soluble in two dimensions, yielding the following values depending on whether or not the test plaquette is inside or outside the current loop:

$$\langle C_{WP}\rangle_{\text{inside}} = \frac{I_0(\beta)}{I_1(\beta)} - \frac{1}{\beta}\ , \tag{3.11a}$$

$$\langle C_{WP}\rangle_{\text{outside}} = \frac{I_1(\beta)}{I_0(\beta)}\ . \tag{3.11b}$$

A periodic 10×10 lattice was used, with $\delta T = 0.01$, $\Delta = 0.1$. At each value of β about 3000 sweeps were carried out for a total evolved Langevin time of 30. This calculation was previously done[6] for large values of β and our agreement with those results is good. At these larger values it is observed that the configurations depart only slightly from the real axis but as β decreases these excursions become larger and larger, thus necessitating the use of the algorithm described above.

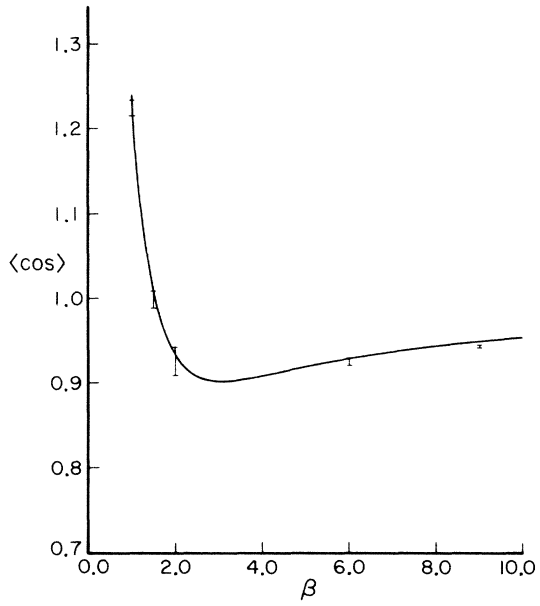

FIG. 2. The average plaquette inside a 5×5 current loop for two-dimensional U(1) lattice gauge theory.

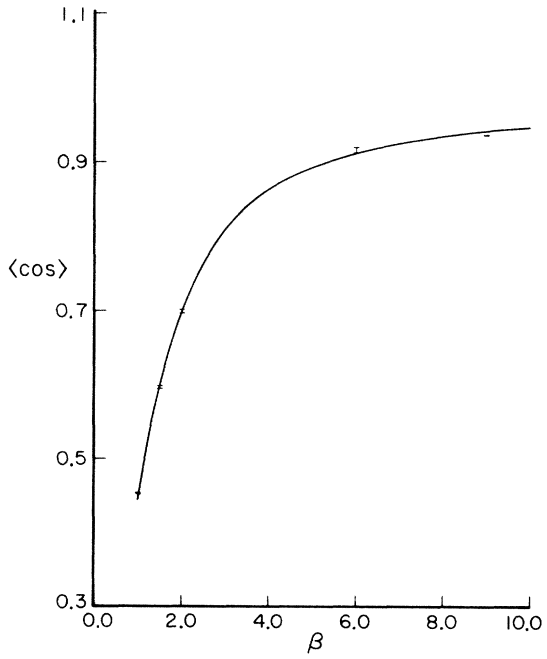

FIG. 3. The average plaquette outside a 5×5 current loop in two-dimensional U(1) lattice gauge theory.

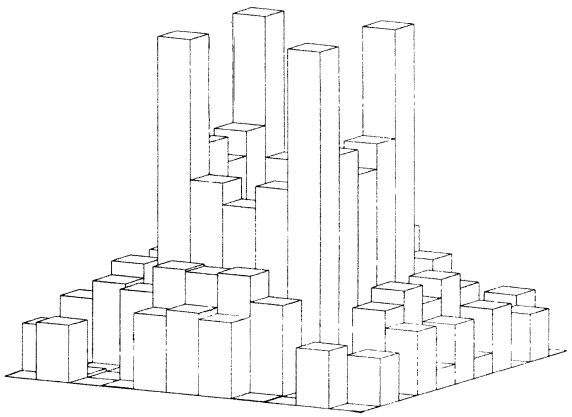

FIG. 4. Plaquette-loop correlations in three-dimensional U(1) lattice gauge theory. 5×5 current loop at $\beta=2$.

The results of simulations in three dimensions are shown in Figs. 4 and 5. This theory is confining for all values of β (Ref. 12) and we chose to calculate at $\beta=2.0$, where the string tension has a significant value[13] and one might expect to find a nontrivial flux tube. The values shown are for the squared parallel electric field density, i.e., for plaquettes lying in the plane of the current loop. Again we work with $\delta T=0.01$ and $\Delta=0.1$. The data for the 5×5 loop correspond to about 5000 sweeps through the system or a total elapsed Langevin time $T=50$. The data for the 7×7 loop have slightly fewer sweeps, around $T=40$. In both cases the relative errors are around 1–2% and it is encouraging that the Langevin time required for equilibration is fairly insensitive to the size of the current loop involved since this means that with only modest computer resources one might hope to study the behavior of the theory at quite large distances.

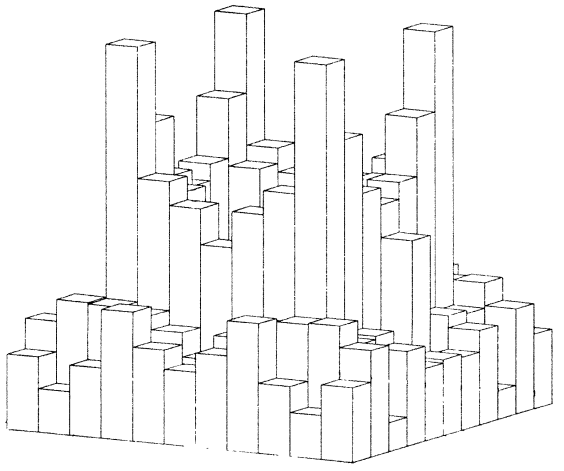

FIG. 5. Plaquette-loop correlations in three-dimensional U(1) lattice gauge theory. 7×7 current loop at $\beta=2$.

IV. NON-ABELIAN GAUGE THEORIES

A crucial question is whether or not this technique is applicable to non-Abelian theories. Previous algorithms, such as the polymer formalism,[14] have proved very successful in the Abelian case but have proved unfeasible in the non-Abelian models.

As a guide to understanding the problems involved we confine attention to the case of SU(2) and study the integral

$$L(\beta)=\frac{\int[dU](\mathrm{Tr}U)^2\exp\left[\frac{\beta}{4}\mathrm{Tr}(U+U^{-1})\right]}{\int[dU]\mathrm{Tr}U\exp\left[\frac{\beta}{4}\mathrm{Tr}(U+U^{-1})\right]}, \quad U\in\mathrm{SU}(2) \tag{4.1}$$

and hence the probability distribution

$$P(U)[dU]=\mathrm{Tr}U\exp\left[\frac{\beta}{4}\mathrm{Tr}(U+U^{-1})\right][dU]\,. \tag{4.2}$$

This is of similar form to the loop-plaquette correlation discussed in Sec. II, but restricted to the case where the lattice has been replaced by a single link.

Using the identity

$$\chi_F{}^2(U)=\chi_A(U)+1 \tag{4.3}$$

for the traces of group elements in the fundamental (F) and adjoint (A) representations one can calculate an analytic expression

$$L(\beta)=\frac{3I_3(\beta)+I_1(\beta)}{4I_2(\beta)}\,. \tag{4.4}$$

Note further that in (4.1) $U^\dagger$ has not been identified with U^{-1}. Although this would be true for the gauge group SU(2) it will not be when we make the complex extension analogous to that used in Sec. II.

To address the problem of the distribution function (4.2) one first constructs the Fokker-Planck equation restricted to the group manifold. To do this introduce covariant derivatives ∇_α which satisfy the same commutation relations as the group generators,

$$[\nabla_\alpha,\nabla_\beta]=i\epsilon_{\alpha\beta\gamma}\nabla_\gamma\,, \tag{4.5}$$

and which can be defined in terms of Pauli matrices by

$$\begin{aligned}&\nabla_\alpha U=\tfrac{1}{2}i\sigma_\alpha U,\quad U\in\mathrm{SU}(2)\,,\\&\nabla_\alpha U^{-1}=-\tfrac{1}{2}iU^{-1}\sigma_\alpha\,.\end{aligned} \tag{4.6}$$

In terms of these derivatives the Fokker-Planck equation corresponding to the distribution $P(U)=e^{-S(U)}$ is

$$\frac{\partial p(U,t)}{\partial t}=\nabla_\alpha\nabla_\alpha p(U,t)-\nabla_\alpha[-p(U,t)\nabla_\alpha S(U)]\,. \tag{4.7}$$

Following Ref. 15, this equation is solved by introducing a discretized Langevin equation for the group elements

$$U(t+\delta t)=U(t)\exp(\delta t\mu+\sqrt{2\delta t}\,\epsilon)\,, \tag{4.8}$$

where, to first order in δt,

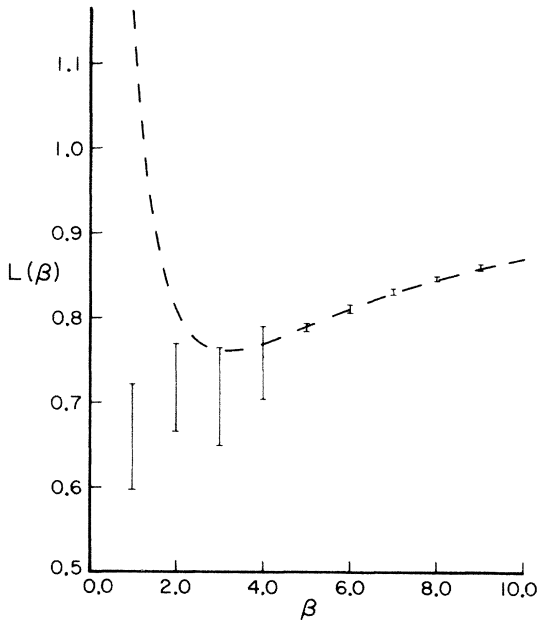

FIG. 6. Numerical calculation of $L(\beta)$, (4.1), according to Eq. (4.10). Comparison with the analytic result, (4.4).

$$\mu = -\nabla_\alpha S(U), \quad \epsilon = \tfrac{1}{2}\sigma\cdot\eta \ , \tag{4.9}$$

and η is a vector of independent normal random numbers with mean zero and unit variance.

In the case where $S(U)$ is real, both μ and ϵ are traceless and anti-Hermitian which is sufficient to guarantee that elements evolving according to (4.7) and (4.8) remain on the SU(2) manifold. However, when $S(U)$ is complex, the matrices μ and ϵ remain traceless, but are no longer anti-Hermitian. This results in the extension of the SU(2) manifold to SL(2,C). The inverse of a matrix is still a well-defined quantity, however, and (4.1) still makes sense, but it is no longer possible to identify $U^\dagger$ with U^{-1}.

Taking these factors into account we can write the discretized Langevin equation corresponding to the distribution (4.2):

$$U(t+\delta t) = U(t)\exp\left[-\tfrac{1}{2}i\delta t\chi(\beta)\cdot\sigma + \left[\frac{\delta t}{2}\right]^{1/2} i\eta\cdot\sigma\right] , \tag{4.10}$$

where

$$\chi_\alpha(\beta) = \left[\frac{\beta}{2} + \frac{1}{\mathrm{Tr}(U+U^{-1})}\right]\mathrm{Tr}[(U-U^{-1})\sigma_\alpha] \ . \tag{4.11}$$

In Fig. 6 are shown the results of simulations of this equation. Obviously the dynamics are faulty at low values of β. Comparing the distributions (3.4) and (4.2) the most obvious difference is that the latter has a zero corresponding to a nonanalyticity in the action, $S(U)$. To study the effect of this zero consider a much simpler integral which admits a simple analytic value:

$$K(\beta) = \frac{\int_0^\pi d\theta \cos^2\theta e^{\beta\cos\theta}}{\int_0^\pi d\theta \cos\theta e^{\beta\cos\theta}} = \frac{I_0(\beta)}{I_1(\beta)} - \frac{1}{\beta} \ . \tag{4.12}$$

We thus attempt to model the distribution function

$$P(\theta)d\theta = \cos\theta e^{\beta\cos\theta}d\theta, \quad 0<\theta<\pi \ . \tag{4.13}$$

Since θ is at this point a purely real variable the conditions of the segregation theorem apply[16] and the zero of $P(\theta)$ divides the interval $[0,\pi]$ into two noncommunicating sectors, $[0,\frac{1}{2}\pi)$ and $(\frac{1}{2}\pi,\pi]$. Thus, if we use the associated SDE

$$d\theta = -(\beta\sin\theta + \tan\theta)dt + \sqrt{2}\,dw(t) \tag{4.14}$$

to generate sample paths of θ and then apply (2.7) to calculate $K(\beta)$ we will arrive at an answer where the integrals have been restricted to one of the above disjoint sectors.

A second possiblity is to make a complex extension of the integrals as before. This is in fact trivial since the range of the integrals in (4.12) can be extended to $[0,2\pi]$ and then the construction of Appendix A applied. The SDE to be solved is now

$$dz = -(\beta\sin z + \tan z)dt + \sqrt{2}\,dw(t) \ , \tag{4.15}$$

which has the same form as (4.14) but for complex z. The conditions of the segregation theorem do not now strictly apply, but another problem exists. In Fig. 7 are shown the trajectories of the deterministic part of (4.15). As can be seen the paths are strongly attracting to the real axis and it is simple to show that once there they never leave. The results of our numerical simulations are shown in Fig. 8 together with the analytic solution, (4.12), and also a numerical evaluation of the integral

$$\frac{\int_0^{\pi/2} d\theta \cos^2\theta e^{\beta\cos\theta}}{\int_0^{\pi/2} d\theta \cos\theta e^{\beta\cos\theta}} \ , \tag{4.16}$$

which is the predicted outcome according to the segregation theorem.

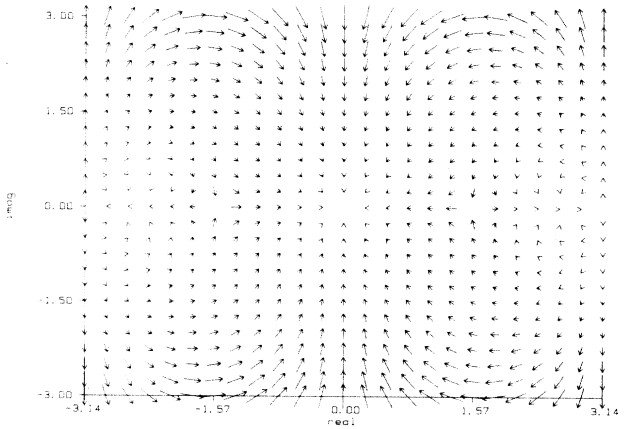

FIG. 7. The trajectories of paths following the deterministic part of the SDE (4.15) showing the attractive nature of the real axis. $\beta = 1.0$.

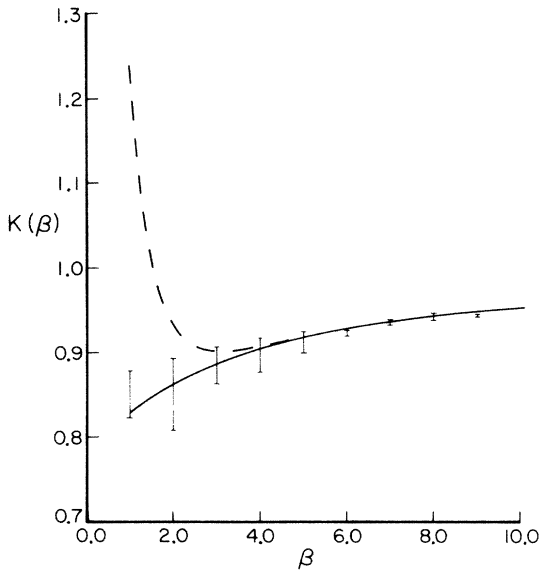

FIG. 8. Numerical calculation of $K(\beta)$, (4.12), according to Eq. (4.15). Comparison with the analytic result (dashed line) and also the ratio of the integrals restricted to the range $[0,\pi/2]$. [(4.16), solid line.]

The agreement with the predictions of this theorem is quite good. This means that our implementation of Eq. (4.7) is inadequate for calculating correlations such as (4.1). This is because the paths, rather than exploring the whole manifold [$\mathbb{C}$ in the case of (4.15) and SL(2,$\mathbb{C}$) for (4.10)], become restricted to smaller manifolds on which the conditions of the segregation theorem apply [$\mathbb{R}$ for (4.15) and SU(2) for (4.10)]. Analytically, this should occur with zero probability, but due to the finite accuracy of our numerical simulations it always occurs in a finite time. This leads to a partitioning of the space into noncommunicating regions between the zeros of the associated distribution function on which, individually, correct results are found but which cannot be used to reproduce the required result.

This is a consequence of the fact that we tried to model actions involving the trace of the large $q\bar{q}$ loop which has a zero. It is probably still possible, however, to use this technique in non-Abelian situations where either no zeros of the intended probability distribution exist or where, by coupling the system to an external field for example, the stability of the paths on the restricted manifold is removed. In these cases the simulations should be ergodic on the extended space and correct results obtained.

Alternatively it may be possible to develop alternative implementations of (4.15) which, by remaining complex, can avoid the segregation problem.

V. CONCLUSION

We have shown that for certain classes of functions, integrals over real fields can be analytically extended to the complex plane. In this form they are amenable to investigation by the techniques of complex SDE's. In particular we have shown that the method is very powerful in the calculation of Abelian lattice gauge theories. The Langevin approach seems to be a viable tool for studying the long-range properties of the theory.

The situation for the non-Abelian theories is, however, less clear. Our conjecture is that the complex Langevin approach will be successful whenever the complex distribution function $P(z)$ does not collapse to a real distribution which has zeros. In particular this means that it may be possible to calculate correlation functions in theories which are coupled to some sort of external field. Similar conclusions have been reached independently.[17]

ACKNOWLEDGMENTS

The authors would like to thank O. Martin, E. Carlen, J. Stack, B. Simon, and J. Franklin for their help with this project which was supported in part by Department of Energy Contract No. DE-FG03-85-ER25009.

APPENDIX A

Consider an entire function $g(z)$ with the property that

$$g(z+2\pi)=g(z), \quad \forall z\in C \; . \tag{A1}$$

Define $I(y)$ to be the integral taken along a contour parallel to the real axis

$$I(y)=\int_{x+iy}^{x+2\pi+iy} dz\, g(z) \; . \tag{A2}$$

Then consider the contour Γ shown in Fig. 9. By the assumed periodicity of $g(z)$ we have

$$\int_B^C dz\, g(z)=\int_A^D dz\, g(z) \tag{A3}$$

and hence by Cauchy's theorem

$$\int_z^{x+2\pi} dx\, g(x+iy)=\int_{x+iy}^{x+2\pi+iy} dx\, g(x+iy) \; . \tag{A4}$$

We have thus shown that $I(y)$ is, in fact, independent of y.

Now consider two functions $f(z)$ and $P(z)$ which satisfy the analyticity and periodicity requirements. Then we have

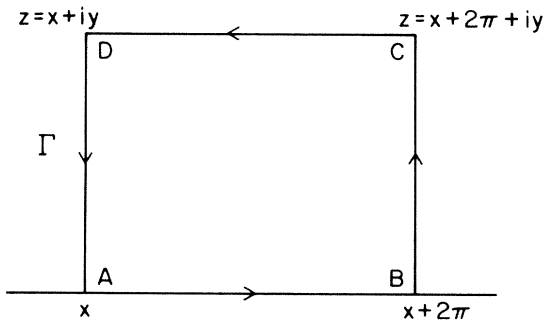

FIG. 9. Contour used in proof of Eq. (A4).

$$\frac{\int_0^{2\pi} dx\, f(x)P(x)}{\int_0^{2\pi} dx\, P(x)} = \frac{\int_{-Y}^{Y} dy \int_0^{2\pi} dx\, f(x)P(x)}{\int_{-Y}^{Y} dy \int_0^{2\pi} dx\, P(x)} \tag{A5}$$

and hence taking the limit $Y \to \infty$ we have that

$$\frac{\int_0^{2\pi} dx\, f(x)P(x)}{\int_0^{2\pi} dx\, P(x)} = \frac{\int_S dz\, f(z)P(z)}{\int_S dz\, P(z)}\ , \tag{A6}$$

where S is any strip of width 2π extending to $\pm\infty$ in the imaginary direction. Now cover the complex plane with such strips and it follows that

$$\frac{\int_0^{2\pi} dx\, f(x)P(x)}{\int_0^{2\pi} dx\, P(x)} = \frac{\int_{\mathbb{C}} dz\, f(z)P(z)}{\int_{\mathbb{C}} dz\, P(z)}\ . \tag{A7}$$

APPENDIX B

For the sake of completeness we present here a formal definition of the segregation theorem as it is used in this paper. The notation used is extensively copied from the original proof of Nagasawa.[16]

Let D be a connected domain in $\mathbf{R}^d$ with a piecewise smooth boundary ∂D defined by

$$\partial D = \{x \in \mathbf{R}^d; P(x) = 0\}\ .$$

Also define X_t, the diffusion process on $D \cap \partial D$, and T, the first exit time for the process from D. Then the segregation theorem states that given a time t_0 and a neighborhood U of the boundary

$$P(T < \infty \text{ or } X_t \in U\ \forall t > t_0) = 0\ .$$

In other words, the probability that the process exits D in a finite time or that it stays permanently "near" the boundary of the domain is zero.

[1] P. de Forcrand, G. Schierholz, H. Schneider, and M. Teper, Phys. Lett. **160B**, 137 (1985).

[2] P. de Forcrand and J. D. Stack, Phys. Rev. Lett. **55**, 1254 (1985).

[3] J. W. Flower and S. W. Otto, Phys. Lett. **160B**, 128 (1985).

[4] J. R. Klauder and W. P. Petersen, J. Stat. Phys. **39**, 53 (1985).

[5] E. Gozzi, Phys. Lett. **150B**, 119 (1985).

[6] J. Ambjorn, M. Flensburg, and C. Peterson, Phys. Lett. **159B**, 335 (1985).

[7] Z. Schuss, *Theory and Application of Stochastic Differential Equations* (Wiley, New York, 1980).

[8] H. Risken, *The Fokker-Planck Equation* (Springer, Berlin, 1984).

[9] T. Kato, *Perturbation Theory for Linear Operators* (Springer, New York, 1966).

[10] J. Ambjorn and S.-K. Yang, Phys. Lett. **165B**, 140 (1985).

[11] H. W. Hamber and Hai-ceng Ren, Phys. Lett. **159B**, 330 (1985).

[12] G. Bhanot and M. Creutz, Phys. Rev. D **21**, 2892 (1980).

[13] J. Ambjorn, A. J. G. Hey, and S. W. Otto, Nucl. Phys. **B210**, 347 (1982).

[14] T. Sterling and J. Greensite, Nucl. Phys. **B220**, 327 (1983).

[15] I. T. Drummond, S. Duane, and R. R. Horgan, Nucl. Phys. **B220**, 119 (1983).

[16] M. Nagasawa, J. Math. Biol. **9**, 213 (1980).

[17] J. Ambjorn, M. Flensburg, and C. Peterson, Lund University Report No. LUTP 86-6, 1986 (unpublished).